

# Role of $^{18}\text{F}$ -FDG PET-CT Imaging in a Patient with Renal Ewing's Sarcoma: A Rare Case Report

<sup>1</sup>Papia Akhter, <sup>1</sup>Tapati Mandal, <sup>2</sup>Pupree Mutsuddy, <sup>3</sup>Md. Abu Bakker Siddique, <sup>4</sup>Shamim M F Begum

<sup>1</sup>Assistant Professor & SMO, National Institute of Nuclear Medicine & Allied Sciences (NINMAS)

<sup>2</sup>Associate Professor & PMO, <sup>3</sup>NINMAS, <sup>3</sup>Professor & CMO - PET-CT Division, NINMAS

<sup>3</sup>Member (Planning division), Bangladesh Atomic Energy Commission

**Correspondence Address:** Dr Papia Akhter, Assistant Professor & SMO, NINMAS, Block-D, BSMMU campus, Shahbag, Dhaka-1000  
Email: papia1078@gmail.com

## ABSTRACT

Ewing's sarcoma (ES) is a bone-related tumor that typically affects young children and adolescents. Primary renal Ewing sarcoma (RES) is extremely rare. Sources of Ewing sarcoma in the kidney include invagination or migration of neural crest cells to the kidney. Here, a case of a young adult male with renal Ewing sarcoma is presented. A 28-year-old male presented with nausea, hematuria, and left flank pain for seven days with an unremarkable previous medical history. An ultrasound and CT scan revealed a massive lobulated mass in the upper and midsection of the left kidney. A radical nephrectomy was done. Histopathology and immunohistochemistry revealed Ewing's sarcoma/primitive neuroectodermal tumor. The chest X-ray and chest CT scan were negative for metastasis. Initial staging was T2bNxM0. Before starting further treatment, the patient was advised to undergo a fluorine- $^{18}\text{F}$ -DG (fluorodeoxyglucose) positron emission tomography ( $^{18}\text{F}$ -FDG PET-CT) scan for the detection of occult metastases. A  $^{18}\text{F}$ -FDG PET-CT scan revealed peritoneal seeding, skeletal and abdominal lymph node metastases. A multimodality workup is essential for proper management of Ewing sarcoma of the kidney due to its rarity and unusual location.  $^{18}\text{F}$ -FDG PET-CT plays a critical role in the detection of occult metastases, staging, restaging, and treatment planning in patients with RES.

**Keywords:** Ewing's sarcoma of kidney,  $^{18}\text{F}$ -FDG PET-CT.

Bangladesh J. Nucl. Med. Vol. 26 No. 1 January 2023

**Doi:** <https://doi.org/10.3329/bjnm.v26i1.64667>

## INTRODUCTION

Primitive neuroectodermal tumors and Ewing's sarcoma (PNET and ES) are more prevalent in children and adolescents and occur in bones and soft tissues. It was first described by Arthur Purdy Stout in 1918 (1). Usually involving the central nervous system, peripheral PNET is very uncommon and has rarely been described in the genitourinary system, including the kidney, urinary bladder, prostate, testis, ovary, and uterus. Renal Ewing sarcoma shows rapid clinical progress and a poor prognosis due to

delayed diagnosis and early-stage metastasis (2, 3). A precise diagnosis for a patient's appropriate management is a great challenge because RES requires more aggressive treatment compared with other primary kidney tumors (4). In the presented case, occult metastases were detected by FDG PET-CT imaging.

## CASE REPORT

A 28-year-old male presented with nausea, hematuria, and left flank pain for seven days. His previous medical history was unremarkable. Physical examination revealed left flank tenderness and a palpable mass. His urine analysis, CBC, and serum creatinine levels were all unremarkable. Ultrasound demonstrated a large, well-defined, mixed echogenic lesion (volume 1336 cc) in the upper pole of the left kidney. A CT scan revealed a massive lobulated mass measuring approximately 13.6 X 14.5 X 12.8 cm in the upper and mid-part of the left kidney, with nodular calcification at the periphery and peripherally enhanced solid component with central necrosis. The mass distorted the kidney and displaced the bowel loops. A radical nephrectomy was done. Histopathology showed an undifferentiated malignant neoplasm. Immunohistochemistry was advised and revealed Ewing's sarcoma/primitive neuroectodermal tumor. Chest radiograph and CT scan were negative for metastasis. Initial staging was T2bNxM0. Before beginning further treatment, the patient was advised to have an FDG PET-CT scan to detect occult metastases.  $^{18}\text{F}$ -FDG PET-CT scan revealed intense FDG avid coeliac, preaortic, paraaortic, splenic hilar, and left common iliac (SUVmax: 15.7) lymph nodes; multiple FDG avid soft tissue density areas along the peritoneum in suprasplenic (SUVmax: 20.7; measuring about 29 X 29

mm) and infrasplic regions, suggesting peritoneal seeding; and FDG avid bony lesions in coracoid process of left scapula, right 3rd, 4th, 7th ribs, D6, D7 vertebrae, ala of sacrum, left iliac bone, right ischium, left pubic bone with involvement of pectinius muscle (SUVmax: 15.1), head, neck and shaft of left femur suggesting skeletal metastases.

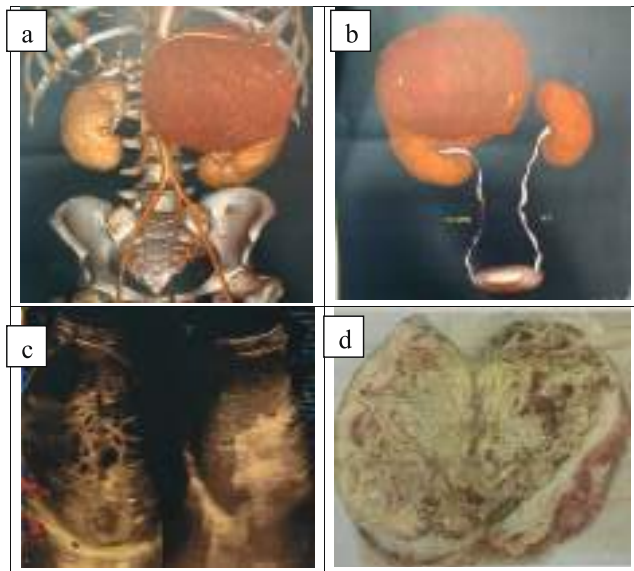


**Figure-a, b:** 3D reconstructed image showing large rounded mass in upper pole of left kidney. **c:** USG showing large heterogeneous mass in left kidney. **d:** Post operative specimen of renal Ewing sarcoma

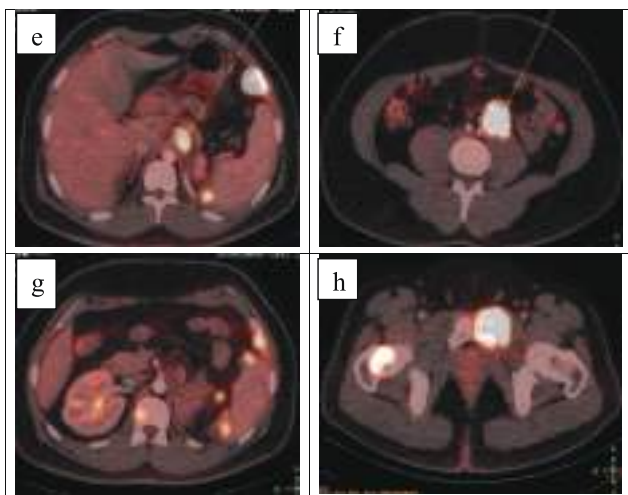


**Figure-e-h:**  $^{18}\text{F}$ -FDG PET-CT scan showing lymph node (e,f), peritoneal (g) and skeletal (h) metastases

## DISCUSSION

PNET/ES is a member of the primitive neuroectodermal tumor family. Its mechanism of development is not known but is similar to that of neuroblastomas. The less accepted

view is that it originates from mesenchymal stem cells (5). RES is extremely rare and might be due to invagination or migration of neural crest cells to the kidney.

RES is usually asymptomatic but produces symptoms when it is larger. These tumors usually have a pseudocapsule, which is usually infiltrated by the tumor (6). The clinical findings are usually complaints of pain (85%), palpable masses (60%), and hematuria (37%). No specific signs of RES have been described in ultrasonography, CT, or MRI. Using ultrasonography, the tumor appears isoechogenic or hyperechogenic to the renal parenchyma. CT findings may show areas of internal hemorrhage or necrosis, peripheral hypervascularity, and diffuse calcification (8). In this reported case, an adult male presented with nausea, hematuria, and left flank pain for seven days with an otherwise unremarkable medical history. Ultrasound demonstrated a large, well-defined mixed echoic lesion (volume 1336 mL) in the upper pole of the left kidney. A CT scan revealed a massive lobulated mass measuring approximately 13.6x14.5x12.8 cm in the upper pole of the left kidney, with nodular calcification at the periphery, predominantly peripherally enhanced solid component, and central necrosis.

The major differential diagnoses for renal RES include a wide range of neoplasms, including malignant lymphoma, renal neuroblastoma, Wilms' tumor, small-cell osteosarcoma, synovial sarcoma, small-cell neuroendocrine carcinoma, and a variant of renal ES with neural differentiation (9, 10). The pathological pictures leading to a diagnosis of PNET/ES are the presence of neurosecretory granules with electron microscopy and the presence of rosettes or pseudorosettes with light microscopy (11). In this case, microscopic examination demonstrated that the tumor was composed of small to medium-sized cells having round and hyperchromatic nuclei with scanty cytoplasm. These cells were arranged in sheets, clusters, and rosette-like structures, pointing to an undifferentiated malignant neoplasm rather than a malignant small, round blue cell tumor, and D/D was a neuroblastoma. CD99 is the most commonly used immunohistochemical stain for the diagnosis of ES and is highly sensitive but not entirely specific (12). NK2.2 is a highly sensitive and moderately specific immunohistochemical marker for ES (13). The specificity of NK2.2 is increased when it is used in

combination with CD99 (14). In this reported case, CD99 and NKX2.2 were positive, which confirmed the diagnosis of Ewing's sarcoma.

The most distinctive feature of the PNET/ESs tissue is that it shows higher glucose metabolism than normal tissues, which is known as the Warburg effect (15). Since this is an aggressive tumor with high metastatic potential, its Warburg effect (SUV) is high due to its high glucose metabolism. So, it is more easily recognized on the <sup>18</sup>F-FDG PET-CT scan. The most common sites of metastasis were the lungs, followed by the liver and bones (2). Franzius and colleagues compared PET and bone scans using <sup>99m</sup>Tc-technetium in their study of 38 patients, where the sensitivity of the bone metastases was determined in patients with PNET and ES. Sensitivity, specificity, and accuracy rates were 100%, 96%, and 97%, respectively, for PET, whereas they were 68%, 87%, and 82% for bone scans. A PET-CT scan is a valuable tool to evaluate the possible site of metastasis. In this case, the patient was advised to have an FDG PET-CT scan to detect occult metastases. <sup>18</sup>F-FDG PET-CT scan revealed intense FDG avid coeliac, preaortic, paraaortic, splenic hilar, and left common iliac (SUVmax: 15.7) lymph nodes; multiple FDG avid soft tissue density areas along the peritoneum in suprasplenic (SUVmax: 20.7; measuring about 29x29 mm) and infrasplenic regions suggesting peritoneal seeding; and FDG avid bony lesions in coracoid process of left scapula, right 3rd, 4th, 7th ribs, D6, D7 vertebrae, ala of sacrum, left iliac bone, right ischium, left pubic bone with involvement of pectinius muscle (SUVmax: 15.1), head, neck and shaft of left femur suggesting skeletal metastases.

The most important step in the management is radical nephrectomy with lymph node dissection. Radiotherapy is used for tumors with positive margins or those extending beyond the Gerota's fascia. Due to occult micrometastases with high recurrence rates and the aggressive potential of the tumor, chemotherapy is usually inevitable. In the reported case, a radical nephrectomy was done, and chemotherapy is in the plan of treatment.

PNETs and ES are very aggressive neoplasms, and early metastasis is their significant characteristic, and 25%–50% demonstrate evidence of metastasis at presentation. The prognosis is poor, with a 5-year disease-free survival rate of

45% to 55% and an overall cure rate of 20% (16). So, early diagnosis and detection of occult metastases are the key factors for proper management.

## CONCLUSION

RES requires more extensive therapy compared with other primary renal neoplasms due to its aggressiveness. Multimodality workup is essential for proper management of Ewing sarcoma of kidney due to its rarity and unusual location. <sup>18</sup>F-FDG PET-CT scan is a valuable tool for detection of metastases and further management as it helps in the detection of disease involvement in tissue even before anatomical changes occur.

## REFERENCES

1. Pomara G, Cappello F, Cuttano MG, et al. Primitive neuroectodermal tumor of the kidney: A case report. *BMC Cancer*. 2004;4:3. doi: 10.1186/1471-2407-4-3.
2. Hakky TS, Gonzalvo AA, Lockhart JL, et al. Primary Ewing sarcoma of the kidney: a symptomatic presentation and review of the literature. *Ther Adv Urol* 2013;5:153–9. Doi:10.1177/1756287212471095
3. Coffin CM, Dehner LP, O'Shea PA. Paediatric soft tissue tumours: a clinical pathological and therapeutic approach. 15 Baltimore, MD, USA: Williams & Wilkins, 1997:80–132.
4. Venkitaraman R, George MK, Ramanan SG, et al. A single institution experience of combined modality management of extra skeletal Ewing's sarcoma. *World J Surg Oncol* 2007;5:3–4. doi:10.1186/1477-7819-5-3
5. Quezado M, Benjamin DR, Tsokos M. EWS/FLI-1 fusion transcripts in three peripheral primitive neuroectodermal tumors of the kidney. *Hum Pathol*. 1997;28:767–71. doi: 10.1016/S0046-8177(97)90147-7
6. Lalwani N, Prasad SR, Vikram R, et al. Pediatric and adult primary sarcomas of the kidney: A cross-sectional imaging review. *Acta Radiologica*. 2011;52:448–57. doi: 10.1258/ar.2011.100376.
7. Angel JR, Alfred A, Sakhujia A, et al. Ewing's sarcoma of the kidney. *Int J Clin Oncol*. 2010;15:314–8. doi: 10.1007/s10147-010-0042-0.
8. Ellinger J, Bastian PJ, Hauser S, et al. Primitive neuroectodermal tumor: Rare, highly aggressive differential diagnosis in urologic malignancies. *Urology*. 2006;68:257–62. doi: 10.1016/j.urology.2006.02.037.
9. Zöllner S, Dirksen U, Jürgens H, et al. Renal ewing tumors. *Ann Oncol* 2013;24:2455–61. doi:10.1093/annonc/mdt215
10. Kang SH, Perle MA, Nonaka D, et al. Primary Ewing sarcoma/PNET of the kidney: fine-needle aspiration, histology, and dual color break apart FISH Assay. *Diagn Cytopathol* 2007;35:353–7. Doi:10.1002/dc.20642
11. Quezado M, Benjamin DR, Tsokos M. EWS/FLI-1 fusion

- transcripts in three peripheral primitive neuroectodermal tumors of the kidney. *Hum Pathol.* 1997;28:767–71. doi: 10.1016/S0046-8177(97)90147-7.
12. Ambros IM, Ambros PF, Strehl S, Kovar H, Gadner H, Salzer-Kuntschik M. MIC2 is a specific marker for Ewing's sarcoma and peripheral primitive neuroectodermal tumors. *Cancer.* 1991; 67: 1886- 1893.
  13. Rooper LM, Sharma R, Gocke CD, Belchis DA. The utility of NKX2.2 and TLE1 immunohistochemistry in the differentiation of Ewing sarcoma and synovial sarcoma [published online ahead of print August 9, 2017]. *Appl Immunohistochem Mol Morphol.* doi:https://doi.org/10.1097/PAI.0000000000000573.
  14. McCuiston A, Bishop JA. Usefulness of NKX2.2 immunohistochemistry for distinguishing Ewing sarcoma from other sinonasal small round blue cell tumors. *Head Neck Pathol.* 2018; 12: 89- 94.
  15. Gillies RJ, Robey I, Gatenby RA. Causes and consequences of increased glucose metabolism of cancers. *J Nucl Med.* 2008;49:24S–42S. doi: 10.2967/jnumed.107.047258.
  16. Angel JR, Alfred A, Sakhuja A, et al. Ewing's sarcoma of the kidney. *Int J Clin Oncol.* 2010;15:314–8. doi: 10.1007/s10147-010-0042-0.